

lysosomes to the cytoplasmic compartment. It should be noted that, although TCRV γ 1.1⁺ T-cell recognition of macrophages correlates with a *Nromp* point mutation, the same TCRV γ 1.1⁺ hybridomas can recognize cells such as P388D tumour cells which do not express the pre-B-cell isoform of *Nromp* (Table 1; Fig. 2*b*; ref. 9). However, these data provide clear evidence that the Bcg locus controls recognition by tumour-reactive $\gamma\delta$ ⁺ cells *in vitro*.

Our data show that TCRV γ 1.1⁺ T cells respond against almost all haematopoietic tumour cells *in vitro* and control growth of two T-cell leukaemias *in vivo*, suggesting that $\gamma\delta$ ⁺ cells mediate tissue-specific tumour immunosurveillance. In addition, we demonstrate that the Bcg locus, which confers innate resistance to intracellular infections, can control $\gamma\delta$ recognition *in vitro* and may link tumour-reactive $\gamma\delta$ T cells to $\gamma\delta$ reactivity against intracellular parasites. □

Received 1 December 1994; accepted 24 March 1995.

1. Klein, G. & Boon, T. *Curr. Opin. Immunol.* **5**, 687–692 (1993).
2. Pardoll, D. M. *Curr. Opin. Immunol.* **5**, 719–725 (1993).
3. Haas, W., Pereira, P. & Tonegawa, S. A. *Rev. Immunol.* **11**, 637–686 (1993).

4. Allison, J. P. & Havran, W. L. A. *Rev. Immunol.* **9**, 679–705 (1991).
5. Raulet, D. H. A. *Rev. Immunol.* **7**, 175–207 (1989).
6. Kronenberg, M. *Curr. Opin. Immunol.* **6**, 64–71 (1994).
7. Ferrick, D. A. et al. *Cell* **57**, 483–492 (1989).
8. Radzioch, D. et al. *J. Leuk. Biol.* **50**, 263–270 (1991).
9. Vidai, S. M., Maio, D., Vogan, K., Skamene, E. & Gros, P. *Cell* **73**, 469–485 (1993).
10. Correa, I. et al. *Proc. natn. Acad. Sci. U.S.A.* **89**, 653–657 (1992).
11. Schild, H. et al. *Cell* **76**, 29–37 (1994).
12. Kärre, K., Ljunggren, H. G., Pirotek, G. & Kiessling, R. *Nature* **319**, 675–678 (1986).
13. O'Brien, R. L. et al. *Cell* **57**, 667–674 (1989).
14. Yeung, R. A. & Elliot, T. J. *Cell* **59**, 5–8 (1989).
15. Silva, C. L., Lukacs, K. & Lowrie, D. B. *Immunology* **78**, 35–42 (1993).
16. Born, W. et al. *Science* **249**, 67–69 (1990).
17. Munk, M. E., Gatrill, A. J. & Kaufmann, S. H. E. *J. Immunol.* **145**, 2434–2439 (1990).
18. Mombaerts, P., Arnoldi, J., Russ, F., Tonegawa, S. & Kaufmann, S. H. E. *Nature* **365**, 53–56 (1993).
19. Kabelitz, D. et al. *J. exp. Med.* **173**, 1331–1338 (1991).
20. De Libero, G. et al. *J. exp. Med.* **173**, 1311–1322 (1991).
21. Uyemura, K. et al. *J. exp. Med.* **174**, 683–692 (1992).
22. Barton, C. H., White, J. K., Roach, T. I. A. & Blackwell, J. M. *J. exp. Med.* **179**, 1683–1687 (1994).
23. Nathan, C. *FASEB J.* **6**, 3051–3061 (1992).

ACKNOWLEDGEMENTS. We thank D. Radzioch, R. A. Yeung, D. Lowrie, G. Klein and the WHO for providing reagents, and P. Ohashi, H. W. Mittrücker, R. Schmits, C. Brunaud, J. L. de la Pempa, M. Mora and D. Siderowski for comments. This work was supported by the National Cancer Institute and Medical Research Council of Canada, the NIH (M.K.), the Crohn's and Colitis Foundation of America (B.S.), and the Austrian Fonds zur Förderung der Wissenschaftlichen Forschung (J.P.).

Furin-dependent intracellular activation of the human stromelysin-3 zymogen

Duanqing Pei & Stephen J. Weiss*

Division of Hematology/Oncology, Department of Internal Medicine, The University of Michigan Comprehensive Cancer Center, Ann Arbor, Michigan 48109-0640, USA

HUMAN stromelysin-3, a new member of the matrix metalloproteinase family, is expressed in tissues undergoing the active remodelling associated with embryonic development, wound healing and tumour invasion^{1–3}. But like all other members of the matrix metalloproteinase gene family, stromelysin-3 is synthesized as an inactive precursor that must be processed to its mature form in order to express enzymic activity^{4,5}. Here we identify stromelysin-3 as the first matrix metalloproteinase to be discovered that can be processed directly to its enzymically active form by an obligate intracellular proteolytic event that occurs within the constitutive secretory pathway. Intracellular activation is regulated by an unusual 10-amino-acid insert sandwiched between the pro- and catalytic-domains of stromelysin-3, which is encrypted with an Arg-X-Arg-X-Lys-Arg recognition motif for the Golgi-associated proteinase, furin, a mammalian homologue of the yeast Kex2 pheromone convertase^{6,7}. A furin–stromelysin-3 processing axis not only differentiates the regulation of this enzyme from all previously characterized matrix metalloproteinases, but also identifies pro-protein convertases as potential targets for therapeutic intervention in matrix-destructive disease states.

Although previously characterized members of the matrix metalloproteinase (MMP) family are secreted as inactive zymogens^{4,5}, COS-7 cells stably transfected with ST3 complementary DNA (COS 4-2) spontaneously expressed ST3 activity and degraded α_1 -proteinase inhibitor (α_1 PI; a substrate for the active MMP⁸). Proteolysis was completely inhibited by tissue inhibitor of metalloproteinase-1 or -2 (TIMP-1 or TIMP-2, respectively) or the synthetic metalloproteinase inhibitor, BB-94 (ref. 9) (Fig. 1*a*). Immunoprecipitation with ST3 polyclonal antisera revealed the presence of two major bands in the conditioned medium of ST3-transfected COS cells with approximate

relative molecular masses of 65K and 45K, respectively (Fig. 1*b*). The 65K species represents the ST3 zymogen, and the 45K species was previously identified as the processed mature form of the enzyme on the basis of an amino terminus homologous to that of the mature form of known MMPs (that is, Phe 98), an intact carboxy terminus, and its ability to cleave the bait region of α_2 -macroglobulin⁸. Importantly, ST3 processing to the active 45K form was similarly observed in ST3-transfected HT-1080 and MCF-7 (Fig. 1*b*) as well as 293, MDCK and CHO cell lines, where the secreted enzyme was recovered only in its mature form ($n = 3$).

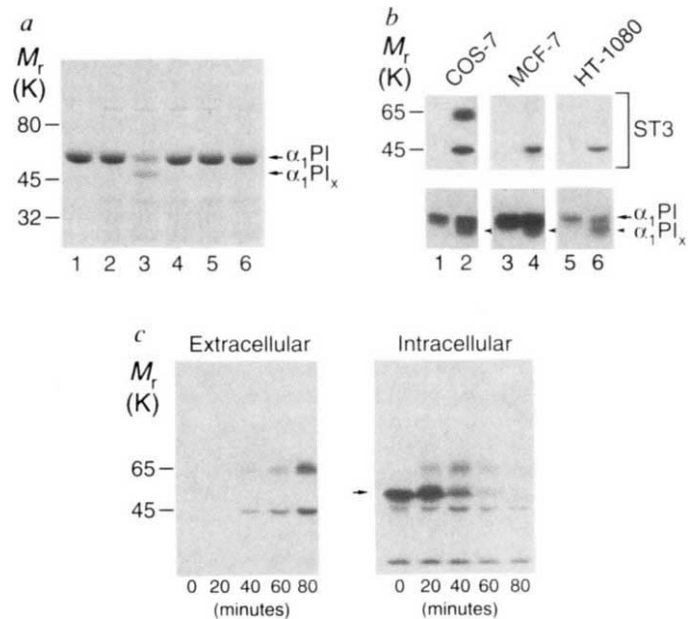
In the extracellular media, pulse-chase analysis of ST3 processing demonstrated that both the 65K zymogen and the 45K active forms of the proteinases were detected in tandem fashion by as early as 40 min post-labelling (Fig. 1*c*). These results are consistent with a rapid extracellular processing event, but the ratio of active ST3 to zymogen did not increase with continued incubation (Fig. 1*c*). Furthermore, the activation of the ST3 zymogen was unaffected by proteinase inhibitors capable of preventing processing of all other MMPs^{4,5} (that is, aprotinin, benzamidine, E-64, α_2 -macroglobulin, TIMP-1/2 or BB-94; data not shown). Although the rapid accumulation of active ST3 in the extracellular milieu and the resistance of the processing event to extracellular antiproteinases are consistent with an intracellular activation cascade, MMPs have been assumed only to undergo activation after secretion^{4,5}. However, when pulse-chase analyses of the intracellular pool of ST3 were examined, the 45K processed form of the proteinase could be detected before its secretion into the extracellular medium (Fig. 1*c*).

The intracellular maturation of the ST3 zymogen suggested that the zymogen displays an encrypted domain that initiates processing. Amino-acid sequence alignments comparing ST3 with other MMPs have identified a non-homologous 10-amino-acid insert that is sandwiched between the pro-domain and the N terminus of the active proteinase¹ (Fig. 2*a*). To determine whether this decapeptide regulates processing, the effect of switching this domain from ST3 to the homologous region in a structurally distinct MMP, human fibroblast collagenase^{1,5} (HFC), was assessed. As expected, although wild-type ST3 was processed to its active form, HFC was secreted as glycosylated and non-glycosylated zymogens⁵ (Fig. 2*a, c*). After domain switching, however, the deletion mutant of ST3 (termed ST3⁻¹⁰) was not processed and secreted only as a single, inactive ~65K species (Fig. 2*b, c*). In contrast, the insertional mutant of HFC (termed HFC⁺¹⁰) was secreted as a fully processed and active

* To whom correspondence should be addressed.

FIG. 1 Activation and processing of ST3. **a**, Detection of ST3 activity. $\alpha_1\text{PI}$ was incubated alone (lane 1), with supernatants from cells stably transfected with the control expression vector (lane 2), or the ST3 expression vector in the absence or presence of rTIMP-1 ($1 \mu\text{g ml}^{-1}$), rTIMP-2 ($1 \mu\text{g ml}^{-1}$) or BB-94 ($5 \mu\text{M}$) (lanes 3–6, respectively) and examined by SDS-PAGE/Coomassie staining. $\alpha_1\text{PI}$, $\alpha_1\text{-proteinase inhibitor}$; $\alpha_1\text{PI}_x$, cleaved $\alpha_1\text{PI}$. **b**, ST3 activation by transfected cell lines. COS, MCF-7 or HT1080 cells transiently transfected with $\alpha_1\text{PI}$ and either the control (lanes 1, 3, 5) or the ST3 expression vector (lanes 2, 4, 6) were analysed by immunoprecipitation with ST3- or $\alpha_1\text{PI}$ -specific polyclonal antisera (upper and lower panels, respectively). The 65K and 45K species are the zymogen and processed forms of ST3, respectively (upper panels). Cleaved $\alpha_1\text{PI}$ is detected when coexpressed with ST3 in all three cell lines (lower panels; lanes 2, 4, 6) but not in control transfected cells (lanes 1, 3, 5). **c**, Pulse-chase analysis of ST3 processing *in situ*. COS-7 cells stably transfected with ST3 were pulse-labelled with [^{35}S]methionine for 5 min and chased with unlabelled methionine for 0 min (lanes 1 and 6), 20 min (lanes 2 and 7), 40 min (lanes 3 and 8), 60 min (lanes 4 and 9) and 80 min (lanes 5 and 10). Supernatants (lanes 1–5) and lysates (lanes 6–10) were immunoprecipitated with anti-ST3 polyclonal antisera. The arrow indicates the position of the non-glycosylated ST3 precursor.

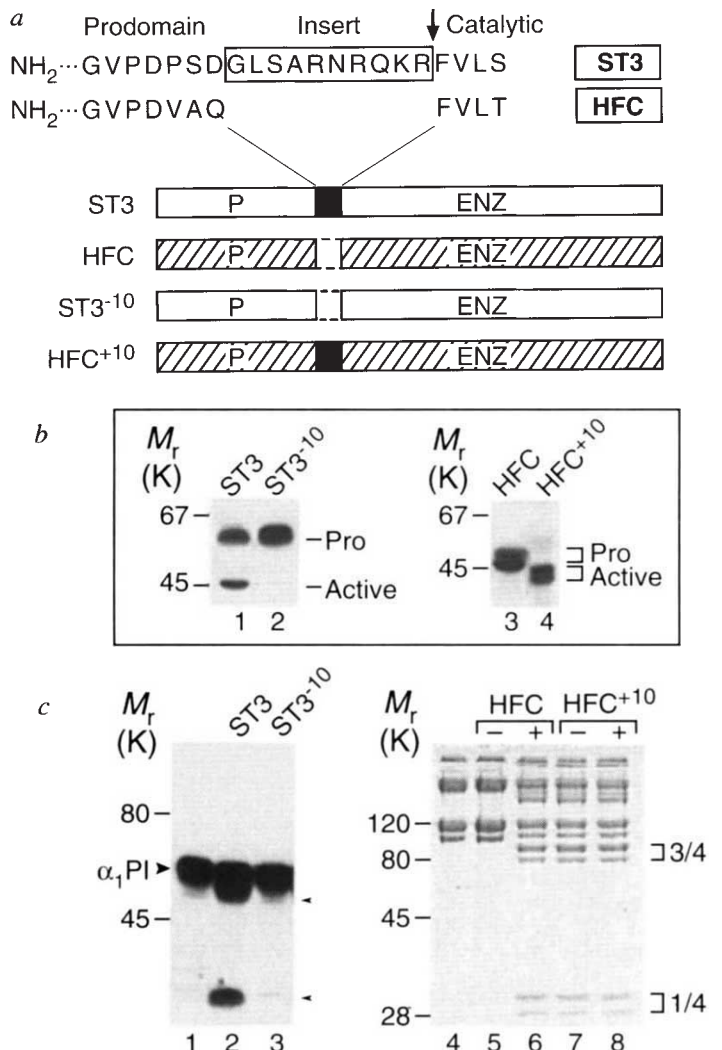
METHODS. COS-7 cells stably transfected with the control or ST3 expression vector have been described previously⁸. Serum-free conditioned media was collected from either cell population and incubated with $\alpha_1\text{PI}$ ($10 \mu\text{g ml}^{-1}$) in the absence or presence of MMP inhibitors for 6 h at 37°C and analysed as described by SDS-PAGE (7.5%)⁸. COS-7, HT-1080 or MCF-7 cells were transiently transfected with the $\alpha_1\text{PI}$ and ST3 expression vectors by LipofectAMINE treatment (BRL-GIBCO) and labelled with [^{35}S]methionine ($100 \mu\text{Ci ml}^{-1}$ for 3 h at 37°C). For pulse-chase analyses, stably transfected COS-7 cells were labelled with



[^{35}S]methionine ($500 \mu\text{Ci ml}^{-1}$) for 5 min and chased with 10 mM unlabelled methionine. Cells were lysed in RIPA buffer²³ in the presence of PMSF, E-64, BB-94 and pepstatin. ST3 and $\alpha_1\text{PI}$ were immunoprecipitated with monospecific polyclonal antisera and processed as described⁸.

FIG. 2 A new 10 amino-acid insert in ST3 encodes an intracellular activation signal. **a**, Schematic representation of domain swaps between ST3 and HFC. The 10 amino-acid insert of ST3 (black box) is located between the pro- (labelled P) and catalytic (labelled ENZ) domains of ST3. ST3⁻¹⁰ is a deletion mutant lacking the insert between residue Asp 87 and Phe 98 whereas HFC⁺¹⁰ contains this motif inserted between residue Gln 99 and Phe 100 (ref. 5). **b**, Processing of ST3 and HFC mutants. ST3 (lane 1), but not ST3⁻¹⁰ (lane 2) was processed to its mature form. In contrast, HFC was secreted as glycosylated and non-glycosylated proforms⁵ (lane 3) whereas HFC⁺¹⁰ was processed completely to the mature enzyme (lane 4). Products were visualized by SDS-PAGE/fluorography after immunoprecipitation. Brackets indicate the glycosylated and non-glycosylated forms of HFC. **c**, Enzymic activities of ST3, ST3⁻¹⁰, HFC and HFC⁺¹⁰. Shown are $\alpha_1\text{PI}$ expressed alone (lane 1) or $\alpha_1\text{PI}$ coexpressed with ST3 (lane 2) or ST3⁻¹⁰ (lane 3). The cleaved $\alpha_1\text{PI}$ products includes the ~50K fragment (upper arrowhead) and the ~4K fragment (lower arrowhead). Native type I collagen (lane 4) was incubated with HFC or HFC⁺¹⁰ (lanes 5 and 7, respectively) or aminophenylmercuric acetate-treated HFC or HFC⁺¹⁰ (lanes 6 and 8, respectively). Although the HFC zymogen expressed no collagenolytic activity until activated with the organomercurial, HFC⁺¹⁰ was secreted as the fully active enzyme. The characteristic 3/4- and 1/4-sized fragments of cleaved type I collagens are indicated.

METHODS. A sequential PCR strategy was used to generate both ST3⁻¹⁰ and HFC⁺¹⁰ (ref. 23). A 5' primer containing the ATG codon and a 3' primer containing the stop codon of ST3 were paired with two complementary internal primers encoding the deletion of the 10 amino-acid insert to generate two partial PCR fragments which were annealed and reamplified to generate ST3⁻¹⁰. HFC⁺¹⁰ was generated in a similar fashion with the following primers: a 5' and a 3' primer of HFC, and two complementary internal primers with a precise insertion of the 10 amino-acid insert of ST3 between Q 99 and F 100 of HFC. The ST⁻¹⁰ and HFC⁺¹⁰ PCR fragments were cloned and sequenced in pCloneAmp (BRL-GIBCO), and cloned into pREP9. DNA transfection and immunoprecipitation was as in Fig. 1a. For N-terminal sequence determination, [^3H]leucine-labelled HFC⁺¹⁰ was immunoprecipitated with specific polyclonal antisera, electrophoresed, immunoblotted and sequenced as described^{8,24}. Collagenolytic activity was analysed after a 12 h incubation with soluble type I collagen at 25°C as described²⁵.



type I collagenase with a new N terminus immediately downstream of the decapeptide at Phe 100 (Fig. 2*b, c*). Thus, despite the fact that HFC displays only limited homology to ST3¹, the 10 amino-acid insert carries all of the information necessary to direct the intracellular processing of the recipient MMP.

The ST3 decapeptide insert contains a tetrad of basic residues arranged in an Arg-X-Arg-X-Lys-Arg sequence (Fig. 2). Interestingly, recent studies indicate that protein precursors that display a triad of basic residues arranged in an Arg-X-Lys/Arg-Arg motif can be cleaved on the C-terminal side of the consensus sequence within the constitutive secretory pathway by mammalian homologues of the yeast processing protease, Kex2 (refs 6, 7). At least six members of the mammalian precursor processing endoproteases have been identified, but only two of these, furin and PACE4, are ubiquitously expressed and display processing activities for constitutively secreted, Arg-X-Lys/Arg-Arg-containing precursors^{6,7}. Sequence rules established for precursor cleavage by furin/PACE4-like convertases indicate critical roles for the basic residues at positions -1, -2 and -4 relative to the scissile bond (that is, P⁻¹, P⁻² and P⁻⁴, respectively)^{10,11}. Thus, the amino-acid sequence requirements for ST3 processing in COS-7 cells¹² were compared in transient transfection assays where the Arg residues at P⁻⁴, P⁻² and P⁻¹ were substituted. In contrast to wild type ST3, Arg→Lys or



FIG. 3 Amino-acid sequence requirements for ST3 processing. The basic residue motif in the 10 amino-acid insert (boxed) of ST3 is shown in bold letters. Mutations were introduced in each of these residues as well as the Phe 98 by a sequential PCR-based strategy. ST3 expression constructs harbouring these mutations were transiently transfected into COS-7 cells and analysed after immunoprecipitation and SDS-PAGE/fluorography as described in Fig. 1.

METHODS. Mutations were introduced into the desired positions in ST3 essentially as described for the generation of ST⁻¹⁰ in Fig. 2. Mutagenic primers used are as follows: R97A, CGCAACCGACAGAAG**CGG**TCGTGCTTTCTGGC; K96D, GCCCGCAACCGACAG**GAT**AGGTTCTGCTTTCT; R94K, CTGAGTGCCCGCAAC**AAG**CAGAAGAGGTTCTGTG; R94A, CTGAGTGCCCGCAAC**CGC**AGAAGAGGTTCTGTG; R92A, GATGGCTGAGTGCC**GCA**AACCGACAGAAGAGG; F98Y, AACCGACAGAAGAG**GAT**GTGCTTTCTGGCGGG. Bold nucleotides indicate the altered codons. These mutagenic primers were paired with the ST3 3' primer to generate C-terminal ST3 fragments carrying the desired mutations by PCR from an ST3 cDNA template⁸. A PCR fragment coding for the pro-domain of ST3 (M1-K96) was generated by amplifying the ST3 cDNA template with the 5' ST3 primer described previously and the primer, CGCTTCTGTCGGTTGCGGGCACTCAGCCATC, whose complementary strand encodes D87-K96. The M1-K96 fragment was annealed to each of the mutated C-terminal ST3 fragment generated above and PCR amplified with the 5' and 3' ST3 primers to generate full-length ST3 mutants as described in Fig. 2. The resulting PCR fragments were cloned into pCloneAmp, screened for mutations by DNA sequencing, and cloned into pREP9 expression vector.

Arg→Ala mutants at P⁻⁴ (R94K and R94A, respectively), Lys→Asp at P⁻² (K96D) or Arg→Ala at P⁻¹ (R97A), were all secreted as unprocessed zymogens (Fig. 3). Although an additional basic residue at P⁻⁶ has not been identified in other Arg-X-Lys/Arg-Arg-containing precursors, mutants containing this extended recognition sequence have been reported to undergo more efficient processing^{10,11,13}. Indeed, an Arg→Ala substitution at P⁻⁶ was processed, but only at a rate ~10% of that

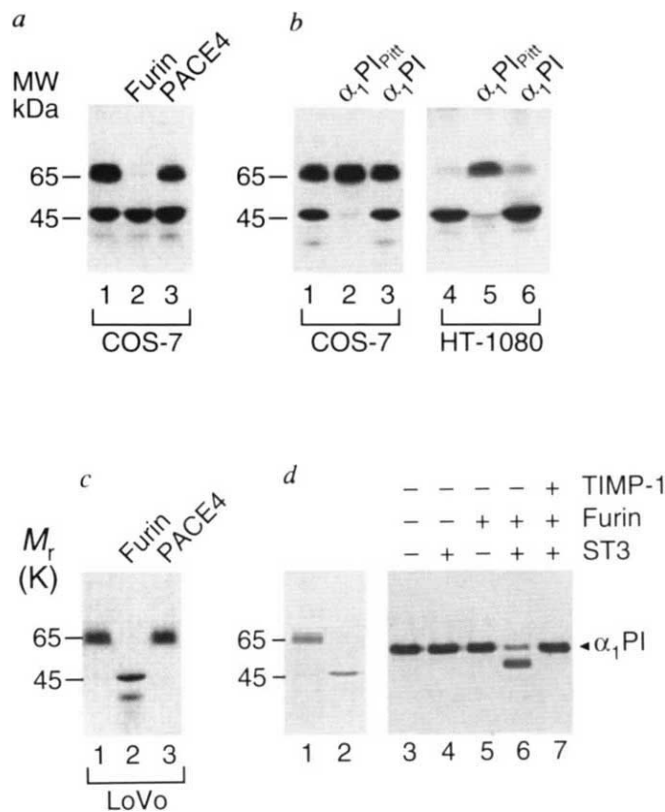


FIG. 4 Processing of ST3 by furin and PACE4. **a**, Efficiency of furin and PACE4 as ST3-processing convertases. ST3 expression vector (1 μ g) was cotransfected with 100 ng control vector (lane 1) or expression vectors for human furin (lane 2) or PACE4 (lane 3) into COS-7 cells. ST3 products were analysed after immunoprecipitation as described in Fig. 1. **b**, Inhibition of ST3 activation by α_1 PI_{in situ}. COS-7 cells (lanes 1–3) or HT-1080 cells (lanes 4–6) were transfected with the following expression vectors; ST3 alone (1 μ g, lanes 1 and 4), ST3 and α_1 PI_{in situ} (1 μ g and 100 ng, respectively; lanes 2 and 5), or ST3 and α_1 PI (1 μ g and 100 ng, respectively; lanes 3 and 6). The ST3 products were analysed following immunoprecipitation as described in Fig. 1. **c**, ST3 processing in the furin-deficient cell line, LoVo. LoVo cells were transfected with expression vector for ST3 (lane 1), or with expression vectors for ST3 and either furin (1 μ g; lane 2) or PACE4 (1 μ g; lane 3). Radiolabelled ST3 products were analysed after immunoprecipitation as described in Fig. 1. **d**, Processing of proST3 by soluble furin under cell-free conditions. ProST3 (50 ng) was then incubated alone (lane 1) or with purified soluble furin (2 units; lane 2) and the mixtures analysed by western blotting with ST3 polyclonal antisera. To assess ST3 proteolytic activity, α_1 PI (200 ng) was incubated alone (lane 3) or with proST3 (20 ng; lane 4), soluble furin (2 units; lane 5), furin-activated ST3 (lane 6) or furin-activated ST3 and TIMP-1 (50 ng; lane 7). Products were analysed by western blotting with α_1 PI polyclonal antisera. **METHODS.** ProST3 was purified from transiently transfected LoVo cells as described⁸. Soluble furin expressed in transiently transfected COS-7 cells was purified and assayed according to ref. 26. Furin-ST3 mixtures were incubated for 2 h at 37 $^{\circ}$ C in 10 mM Tris-HCl, 250 mM NaCl, 1 mM CaCl₂ and 0.02% Brij 35 (pH 7.0). N-terminal sequence analysis of furin-processed ST3 was determined as described⁸ in the absence or presence of BB-94. α_1 PI hydrolysis was determined under conditions in Fig. 1 and the antiproteinase immunoblotted with polyclonal antisera (Calbiochem) as described⁸.

observed with the wild-type proteinase (Fig. 3). Finally, given that substitutions in the P⁺ position are more readily tolerated^{10,11}, F98Y was processed comparably to wild-type ST3 (Fig. 3). Under the assumption that insert substitutions did not significantly perturb the conformation of the Arg 97-Phe 98 cleavage site^{12,14}, these results suggest that ST3 undergoes furin- or PACE4-mediated processing.

To assess the relative efficiency of furin versus PACE4 in ST3 processing, COS-7 cells were cotransfected with ST3 cDNA and either furin or PACE4 cDNAs (Fig. 4a). Although COS cells transfected with either pro-protein convertase express the respective proteases comparably¹², only furin increased ST3 processing (Fig. 4a). Furthermore, when ST3-transfected COS-7 or HT-1080 cells were cotransfected with the Pittsburgh mutant of α_1 PI (α_1 PI_{Pitt}), a reactive site variant that inhibits furin (but not PACE4) activity *in situ*^{12,14}, ST3 processing was completely blocked (Fig. 4b). Consistent with these findings, LoVo cells, a carcinoma cell line that does not produce functional furin¹⁵, were unable to process the ST3 zymogen to its active form (Fig. 4c). However, when LoVo cells were cotransfected with ST3 and furin (but not PACE4) cDNAs, processing was reestablished (Fig. 4c). Finally, to determine whether furin directly mediates ST3 processing, a soluble form of the convertase was generated by deleting the transmembrane domain^{12,14} and the purified mutant incubated with the ST3 zymogen under cell-free conditions. At neutral pH, the soluble furin mutant efficiently cleaved the ST3 zymogen at the Arg 97-Phe 98 junction (as determined by N-terminal sequencing) to generate the active 45K form of the proteinase (Fig. 4d).

We have demonstrated that ST3 is processed directly to its mature active form by the pro-protein convertase, furin. A mammalian homologue of the yeast Kex2 pheromone convertase, furin is a transmembrane serine proteinase concentrated in the *trans*-Golgi network^{6,7,16,17}. Furin efficiently processes serum proteins, growth factors and membrane receptors containing an Arg-X-Lys-Arg sequence^{6,7}, but an additional Arg residue at P⁻⁶ was necessary for the efficient processing of the ST3 zymogen. Apparently, the inclusion of this enhancing signal for human ST3 processing is evolutionarily conserved because mouse² and *Xenopus*¹⁸ ST3 homologues each contain the identical motif. Importantly, a new transmembrane MMP that controls gelatinase A activation also contains a decapeptide insert with an Arg-X-Lys-Arg motif upstream of its catalytic domain^{19,20}. Thus, we propose that pro-protein convertases may serve as important regulators of multiple metalloproteinases involved in extracellular matrix turnover. The unexpected identification of furin as an activator of MMPs that are strongly implicated in tumour progression suggests that recently developed pro-protein convertase inhibitors^{21,22,27} might be developed as anti-cancer therapeutics. □

19. Sato, H. *et al.* *Nature* **370**, 61–65 (1994).
20. Cao, J., Sato, H., Takino, T. & Seiki, M. *J. Biol. Chem.* **270**, 801–805 (1995).
21. Hallenberger, S. *et al.* *Nature* **360**, 358–361 (1992).
22. Decroly, E. *et al.* *J. Biol. Chem.* **269**, 12240–12247 (1994).
23. Ausubel, F. M. *et al.* (eds) *Curr. Prot. molec. Biol.* (Wiley, New York, 1994).
24. Birken, S., Fetherston, J., Canfield, R. & Boime, R. *J. Biol. Chem.* **256**, 1816–1823 (1981).
25. Desrochers, P. E., Mookhtiar, K., Van Wart, H., Hasty, K. A. & Weiss, S. J. *J. Biol. Chem.* **267**, 5005–5012 (1992).
26. Bravo, D. A., Gleason, J. B., Sanchez, R. I., Roth, R. A. & Fuller, R. S. *J. Biol. Chem.* **269**, 25830–25837 (1994).
27. Anderson, E. A., Thomas, L., Hayflick, J. S. & Thomas, G. *J. Biol. Chem.* **268**, 24887–24891 (1993).

ACKNOWLEDGEMENTS. We thank A. Rehemtulla and R. Kaufman (HHMI, University of Michigan) for pro-peptide convertase, α_1 PI, α_1 PI_{Pitt}, and soluble furin expression vectors as well as helpful discussions, R. Fuller (University of Michigan) for guidance in purifying soluble furin, A. Galloway (British Biotechnology) for BB-94, C. Thompson (Synergen) for rTIMP-1, K. Langley (Amgen) for rTIMP-2 and H. Welgus for HFC polyclonal antisera. D.P. was supported in part by an Oncology Research Training Grant from the National Heart, Lung and Blood Institute. This study was supported by grants from the University of Michigan Cancer Research Committee, the Michigan Breast Care Center, the Charlotte Geyer Foundation and the US Army Medical Research Command.

Direct stimulation of Jak/STAT pathway by the angiotensin II AT₁ receptor

Mario B. Marrero*, Bernhard Schieffer*, William G. Paxton†, Lauri Heerdt‡, Bradford C. Berk‡, Patrick Delafontaine§ & Kenneth E. Bernstein*||

Departments of * Pathology and Laboratory Medicine, and § Medicine, Division of Cardiology, Emory University, Atlanta, Georgia 30322, USA

† Santa Cruz Biotechnology Inc., Santa Cruz, California 95060, USA

‡ Department of Medicine, Division of Cardiology, University of Washington, Seattle, Washington 98195, USA

THE peptide angiotensin II is the effector molecule of the renin-angiotensin system. All the haemodynamic effects of angiotensin II, including vasoconstriction and adrenal aldosterone release, are mediated through a single class of cell-surface receptors known as AT₁ (refs 1, 2). These receptors contain the structural features of the G-protein-coupled receptor superfamily³. We show here that angiotensin II induces the rapid phosphorylation of tyrosine in the intracellular kinases Jak2 and Tyk2 in rat aortic smooth-muscle cells and that this phosphorylation is associated with increased activity of Jak2. The Jak family substrates STAT1 and STAT2 (for signal transducers and activators of transcription) are rapidly tyrosine-phosphorylated in response to angiotensin II. We also find that Jak2 co-precipitates with the AT₁ receptor, indicating that G-protein-coupled receptors may be able to signal through the intracellular phosphorylation pathways used by cytokine receptors^{4,5}.

To investigate whether angiotensin II (Ang II) stimulates Jak2 phosphorylation, rat aortic smooth-muscle (RASM) cells were exposed to Ang II, and Jak2 tyrosine-phosphorylation was measured by two methods. In the first, cell lysates were immunoprecipitated with a monoclonal anti-phosphotyrosine antibody, precipitated proteins were separated by gel electrophoresis, transferred to nitrocellulose and then immunoblotted with a polyclonal anti-Jak2 antibody (Fig. 1a). In the second protocol, the order of antibody addition was reversed: the cell lysate was immunoprecipitated with anti-Jak2 and then immunoblotted with anti-phosphotyrosine (Fig. 1b). Similar experiments were done in parallel in which RASM cells were exposed to murine interferon (IFN)- γ , a cytokine that activates phosphorylation of Jak2 (Fig. 1c)^{4,5}. Within 5 min of exposure to Ang II, tyrosine

Received 30 January; accepted 22 March 1995.

1. Basset, P. *et al.* *Nature* **348**, 699–704 (1990).
2. Lefebvre, O. *et al.* *J. Cell Biol.* **119**, 997–1002 (1992).
3. Wolf, C. *et al.* *Proc. natn. Acad. Sci., U.S.A.* **90**, 1843–1847 (1993).
4. Matrisian, L. M. *BioEssays* **14**, 455–463 (1992).
5. Birkedal-Hansen, H. *et al.* *Crit. Rev. Oral Biol. Med.* **4**, 197–250 (1993).
6. Steiner, D. F., Smeekens, S. P., Ohagi, S. & Chan, S. J. *J. Biol. Chem.* **267**, 23435–23438 (1992).
7. Seidah, N. G., Day, R. & Chretien, M. *Biochem. Soc. Trans.* **21**, 685–691 (1993).
8. Pei, D. Q., Majumdar, G. & Weiss, S. J. *J. Biol. Chem.* **269**, 25849–25855 (1994).
9. Davies, B., Brown, P. Q., East, N., Crimmin, M. J. & Balkwill, E. R. *Cancer Res.* **53**, 2087–2091 (1993).
10. Watanabe, T. *et al.* *J. Biol. Chem.* **267**, 8270–8274 (1991).
11. Watanabe, T., Murakami, K. & Nakayama, K. *FEBS Lett.* **320**, 215–218 (1993).
12. Rehemtulla, A. & Kaufman, R. *J. Biol. Chem.* **269**, 2349–2355 (1992).
13. Liu, Y.-C. *et al.* *Proc. natn. Acad. Sci., U.S.A.* **90**, 8957–8961 (1993).
14. Wasley, C. L., Rehemtulla, A. & Kaufman, R. J. *J. Biol. Chem.* **268**, 8458–8465 (1993).
15. Tsuneoka, M. *et al.* *J. Biol. Chem.* **268**, 26461–26465 (1993).
16. Molloy, S. S., Thomas, K. J., Van Slyke, K., Stenberg, P. E. & Thomas, G. *EMBO J.* **13**, 18–33 (1994).
17. Vidricaire, J., Denault, J.-B. & Leduc, R. *Biochem. biophys. Res. Commun.* **195**, 1011–1018 (1993).
18. Patterson, D., Hayes, W. P. & Shi, Y. B. *Devl Biol.* **167**, 252–262 (1995).

To whom correspondence should be addressed.